PHYSICAL REVIEW B VOLUME 6, NUMBER 10 15 NOVEMBER 1972

Anisotropy of the Electron-Phonon Interaction in Copper*

David Nowak†

The James Franck Institute and the Department of Physics, The University of Chicago, Chicago, Illinois 60637

(Received 23 March 1972)

Absolute values of the anisotropy of the electron-phonon renormalization and of the anisotropy of the temperature-dependent (T^3) component of the quasiparticle scattering rate on the Fermi surface of copper have been calculated. The electron-phonon matrix element is expressed in terms of an augmented-plane-wave (APW) phase-shift pseudopotential. The anisotropies of the Fermi surface, the phonon spectrum, and the wave functions of the initial and final states are explicitly taken into account. The results are compared with experimental data on the scattering rate of quasiparticles by thermal phonons in copper. The calculation predicts an anisotropic variation of the absolute scattering rate which is in good over-all agreement with the experimental data. It is found that the large increase on the scattering rate on the necks can be explained by taking into account the scattering of electrons by transverse phonons. The predicted anisotropy of the renormalization factor is in good agreement with that obtained from a phenomenological interpretation of experimental cyclotron-mass data. The results of this paper suggest the applicability of the APW pseudopotential to the description of the electron-phonon interaction in other metals of the transition series.

I. INTRODUCTION

The anisotropy of the electron-phonon interaction in copper has been demonstrated in several recent experiments. The earliest is that by Häussler and Welles,[1] who, by measuring the damping of cyclotron resonance curves, were able to estimate the temperature-dependent (T^3) component of the quasiparticle relaxation time for certain orbits on the Fermi surface. More recently Koch and Doezema[2] have measured the relaxation time in various symmetry zones on the Fermi surface through surface-quantum-state resonance experiments, and Gantmakher[3] has measured the relaxation time averaged over various orbits by the radio-frequency size effect. All of these experiments show a distinct anisotropy of the T^3 component of the relaxation time, which can be attributed to the scattering of quasiparticles by thermally excited phonons. The reported values of the relaxation time vary by a factor of about 30 over the Fermi surface. A review of all but the most recent experimental work on the anisotropy of the relaxation time in the noble metals has been given by Springford.[4] There are no direct experimental measurements of the anisotropy of the effective-mass enhancement, but Lee[5] has interpreted experimental cyclotron-mass data to deduce the anisotropy of electron-phonon contribution to the mass enhancement, and he found a variation of the enhancement by a factor of about 4 over the Fermi surface.

Although there are no first-principles calculations of the anisotropy of the above quantities, Allen[6] has calculated the Fermi-surface average of the electron-phonon mass enhancement in the noble metals. His approach is that which has been so successful for the nontransitions metals: using a single plane-wave pseudopotential to describe the electron-phonon interaction and neglecting the anisotropies of the Fermi surface and the phonon spectrum. He found than an empirically based pseudopotential of Fong and Cohen[7] yields a Fermi-surface average of the mass enhancement factor that is consistent with other evidence. The purpose of this paper is to present a first-principles calculation of both the anisotropy of the mass enhancement and the temperature-dependent quasiparticle relaxation time. In such a calculation it is necessary to consider all the anisotropies in the problem: that of the Fermi surface, the wave functions, the density of states, and the phonon spectrum.

If the lattice potential were negligible, the Fermi surface of copper would be spherical and would lie entirely within the first Brillouin zone. In fact, the electron-lattice interaction causes the Fermi surface to bulge along the $\langle 100\rangle$ and $\langle 111\rangle$ directions and to intersect the zone boundary along the $\langle 111\rangle$ direction, forming necks. It is in the $\langle 100\rangle$ and $\langle 111\rangle$ directions that the mass enhancement and the quasiparticle scattering rate achieve their largest values.

The necks in copper are associated with the filled d bands which lie a few electron volts below the Fermi energy. The proximity of the d bands to the Fermi surface invalidates the small-core approximation of pseudopotential theory. However, recent work has shown that an accurate model of the Fermi surface can be obtained by phase-shift analysis.[8] The method consists of representing the lattice potential by a spherically symmetric potential of muffin-tin form centered on each of the lattice sites, and a constant potential in the interstitial region. The muffin-tin potential can be described by a set of phase shifts $\eta_l(E_F)$, which

are determined by fitting experimental Fermi-surface data. In this way a model of the Fermi surface of copper accurate to about 1 part in 10^4 has been constructed,[8] and the phase-shift model has been used to calculate the band-structure velocities over the Fermi surface with a computational accuracy of about 0.2%.[5] In the present work this method is extended to calculate the wave functions at various points on the Fermi surface.

The phonon spectrum for copper was obtained from the inelastic-neutron-scattering data of Nicklow *et al.*,[9] which yielded phonon frequencies for wave vectors along principal symmetry directions. Nicklow *et al.* fitted a Born–von Kármán interatomic-force-constant model to their data. This model was used to calculate the phonon frequencies and polarizations in off-symmetry directions.

The application of the APW method to the electron-phonon interaction has been discussed by several authors. Golibersuch[10] and Sinha[11] have investigated the general form of the matrix element, and more recently Allen and Lee[12] have related it to the phase-shift method and have studied its applications to the alkali metals. In this paper the APW formulation of the electron-phonon matrix element is extended to take into account the anisotropies of the initial and final states, and is applied to the calculation of the mass enhancement and the quasiparticle-scattering rate in copper.

This paper is divided into five sections. In Sec. II the theory of the electron-phonon renormalization and the quasiparticle scattering rate is discussed. Section III is devoted to the evaluation of the electron-phonon matrix element and its dependence on the initial and final states. In Sec. IV the calculations of the mass enhancement $\lambda(\vec{k})$ and the relaxation time $\tau(\vec{k})$ are presented, and compared with other theoretical and experimental values. The results and conclusions are summarized in Sec. V.

II. THEORY

A. Renormalization

The electron-phonon interaction influences the quasiparticle energy spectrum only within a width $\pm\hbar\omega_D$ of the Fermi energy, where ω_D is the Debye frequency. The perturbed quasiparticle energy can be expressed as[13]

$$E_{\vec{k}} = \epsilon_{\vec{k}} + \Sigma_{\text{el-ph}}(E_{\vec{k}}, \vec{k}) \ , \tag{1}$$

where $\epsilon_{\vec{k}}$ is the unperturbed energy and includes the effects of the band structure and the electron-electron interaction; $\epsilon_{\vec{k}}$ and $E_{\vec{k}}$ are measured from the Fermi energy. The second term is the electron-phonon proper self-energy of the quasiparticle.

For small $E_{\vec{k}}$ (i.e., $E_{\vec{k}} \ll \hbar\omega_D$), $\Sigma_{\text{el-ph}}$ is proportional to $E_{\vec{k}}$; we define this constant of proportionality as $-\lambda(\vec{k})$. Thus for small $E_{\vec{k}}$ the quasiparticle excitation spectrum is given by

$$E_{\vec{k}} = \epsilon_{\vec{k}}/[1+\lambda(\vec{k})] \ . \tag{2}$$

It is clear from Eq. (2) that any physical observable which depends linearly on a derivative of the quasiparticle energy at the Fermi surface will be renormalized by the factor $[1+\lambda(\vec{k})]$. In particular, the local quasiparticle velocity $\nabla_{\vec{k}_\perp} E_{\vec{k}}$ and the local density of states $D(E_{\vec{k}}, \vec{k})$ will be modified as follows:

$$v_{\vec{k}} = \nabla_{\vec{k}_\perp} E_{\vec{k}} = \nabla_{\vec{k}_\perp} \epsilon_{\vec{k}}/[1+\lambda(\vec{k})] \ , \tag{3}$$

$$D(E_{\vec{k}}, \vec{k}) = D^0(\epsilon_{\vec{k}}, \vec{k})\,[1+\lambda(\vec{k})] \ , \tag{4}$$

where $\vec{k}_\perp$ is the component of $\vec{k}$ normal to the Fermi surface.

The electron-phonon self-energy has been discussed by several authors, and we shall not go into detail here.[14,15] The real part of the self-energy describes the contribution of the absorption and emission of virtual phonons to the quasiparticle energy, whereas the imaginary part is related to the decay of quasiparticle excitations due to the interaction with thermal phonons.

The renormalization factor can be expressed as

$$\lambda(\vec{k}) = \frac{2\Omega}{(2\pi)^3} \sum_\sigma \int \frac{dS_{\vec{k}'}}{\hbar v_{\vec{k}'}} \frac{|M^{\sigma}_{\vec{k},\vec{k}'}|^2}{\hbar\omega^{\sigma}_{\vec{k},\vec{k}'}} \ , \tag{5}$$

where Ω is the volume of the primitive unit cell, and σ is the polarization of the phonon with wave vector $\vec{k}-\vec{k}'$ and frequency $\omega^{\sigma}_{\vec{k}\vec{k}'}$. The integral is over the Fermi surface and is weighted by the inverse velocity, which is a measure of the local density of states. $|M^{\sigma}_{\vec{k}\vec{k}'}|$ is the matrix element for scattering an electron from state $\vec{k}$ to state $\vec{k}'$.

B. Relaxation Time

The inverse lifetime $\hbar/\tau(\vec{k})$ of quasiparticle excitations, due to scattering by thermal phonons, is equal to twice the imaginary part of the electron-phonon self-energy. The scattering rate is dependent on both the energy of the quasiparticle, as measured from the Fermi energy, and the wave vector. The general expression for inverse lifetime is[15]

$$\frac{\hbar}{\tau(E_{\vec{k}}, \vec{k})} = \frac{\Omega}{(2\pi)^2} \sum_\sigma \int \frac{dS_{\vec{k}'}}{\hbar v_{\vec{k}'}} |M^{\sigma}_{\vec{k}\vec{k}'}|^2 \,[2N(\omega) + 1 - f(E-\omega) + f(E+\omega)], \tag{6}$$

where N and f are Bose-Einstein and Fermi-Dirac distributions, respectively, and ω is the frequency of the phonon of wave vector $\vec{k}-\vec{k}'$. We are interested in the lifetime of quasiparticles at the Fermi surface in the limit $T \to 0$. At finite temperatures, however, the Fermi surface is smeared out and,

as pointed out by Allen,[16] it is necessary to evaluate the thermal average of the inverse lifetime, which is given by

$$\frac{\hbar}{\tau(0,\vec{k})} = \int d\epsilon \left(\frac{-\partial f}{\partial \epsilon}\right) \frac{\hbar}{\tau(\epsilon,\vec{k})} . \quad (7)$$

In the limit $T \to 0$, this has the effect of increasing the inverse lifetime by the isotropic factor $\frac{12}{7}$. The general result for $\langle \hbar/\tau(0, \vec{k})\rangle$ is

$$\frac{\hbar}{\tau(\vec{k})} \equiv \left\langle \frac{\hbar}{\tau(0,\vec{k})} \right\rangle = \frac{2\Omega}{(2\pi)^2} \sum_\sigma \int \frac{dS_{\vec{k}'}}{\hbar v_{\vec{k}'}} |M^\sigma_{\vec{k}\vec{k}'}|^2 \{N(\omega)[N(\omega)+1]\} . \quad (8)$$

For $T \ll \Theta_D$, where Θ_D is the Debye temperature, the above expression is dominated by small-angle scattering, and in the low-temperature limit it reduces to:

$$\frac{\hbar}{\tau(\vec{k})} = \sum_\sigma \frac{2k_B^3\Omega}{M\pi\hbar^3 v_{\vec{k}}} \frac{12}{7} \zeta(3) \left\langle \frac{|V^\sigma(0,\vec{k})|^2}{C_\sigma^4} \right\rangle T^3 , \quad (9)$$

where M is the mass of the ion and k_B is the Boltzmann constant. $\zeta(3)$ is the Riemann ζ function and $\langle\rangle$ signifies the angular average of the quantity enclosed. C_σ is the velocity of sound for a long-wavelength phonon of polarization σ. $V^\sigma(0, \vec{k})$ is the $q \to 0$ limit of the pseudopotential, which is given by

$$|V^\sigma(0,\vec{k})|^2 = \lim_{\vec{k}'\to\vec{k}} \frac{2M\omega^\sigma_{\vec{k}\vec{k}'}}{\hbar|\vec{k}-\vec{k}'|^2} |M^\sigma_{\vec{k}\vec{k}'}|^2 . \quad (10)$$

In the above expression $\vec{k}$ and $\vec{k}'$ are restricted to lie on the Fermi surface.

The anisotropic quantities in Eq. (9) are the velocity $v_{\vec{k}}$, the velocity of sound C^σ, and the matrix element $|M^\sigma_{\vec{k}\vec{k}'}|$. The first two of the quantities vary by factors of no more than 2 over the Fermi surface, while the experimental value of $\hbar/\tau(\vec{k})$ varies by a factor of about 30. Thus, to explain this anisotropy, it is necessary that the matrix element be highly anisotropic. This will be shown to be the case.

In the calculation of $\lambda(\vec{k})$ and $\hbar/\tau(\vec{k})$ it is necessary to use accurate models for the anisotropy of the band velocity, the Fermi surface, the phonon spectrum, and the electron-phonon matrix element $|M^\sigma_{\vec{k}\vec{k}'}|$. The band velocity was determined from energy bands calculated from a modified Chodorow potential, which is believed to include the dominant effects of the electron-electron interaction.[8]

The Fermi-surface radii were obtained by fitting an APW phase-shift expansion to experimental de Haas–van Alphen data, for various extremal orbits normal to symmetry directions. In this way it was possible to obtain Fermi-surface radii, which are accurate to within the experimental limit of error. The details of the calculation of band velocities and the Fermi-surface radii are given in Ref. 8.

A Born–von Kármán atomic-force-constant model was used to calculate the phonon spectrum for arbitrary wave vectors. The model took into account six shells of nearest neighbors and assumed the force constants to be axially symmetric. This restriction was necessary, as the parameters were determined from inelastic-neutron-scattering data along principal symmetry directions, and the parameters of the general sixth-order nearest-neighbor model cannot be determined uniquely from symmetry data alone. The force constants used are those reported by Nicklow *et al.* and set out in Table I. The phonon spectrum was determined by solving the normal-mode equation

$$M\omega^2 \xi_\alpha = \sum_\beta \xi_\beta D_{\alpha\beta}(\vec{q}) , \quad (11)$$

where M is the mass of the ion, ω is the phonon frequency, and ξ_α, ξ_β are the Cartesian components of the polarization vectors. The dynamical matrix is given by

$$D_{\alpha\beta}(\vec{q}) = \sum_{L\neq 0} [-\varphi_{\alpha\beta}(\vec{R}_L)][1-\cos(\vec{q}\cdot\vec{R}_L)] , \quad (12)$$

where the $\vec{R}_L$ are the lattice coordinates of the nearest-neighbor atoms, here restricted to sixth-order neighbors, and $\varphi_{\alpha\beta}$ are the atomic force constants set out in Table I.

The analytical expression for the electron-phonon matrix element is discussed in detail in Sec. III. The anisotropy of the matrix element will be shown to depend on the magnitude of the initial- and final-state wave vectors, and on the actual form of the wave function of the initial and final states.

III. ELECTRON-PHONON MATRIX ELEMENT

The matrix element of the electron-phonon interaction can be formulated by replacing the actual lattice potential perturbed by phonons with an array of appropriately displaced "muffin-tin" po-

TABLE I. Atomic force constants for the sixth-order nearest-neighbor model used in the calculation of the phonon spectrum.

	Atomic force constants (Ref. 9) (dyn/cm)		
$\varphi_{xx}(1)$	13 278	$\varphi_{xx}(4)$	350
$\varphi_{zz}(1)$	−1 351	$\varphi_{zz}(4)$	−327
$\varphi_{xy}(1)$	14 629	$\varphi_{xy}(4)$	677
$\varphi_{xx}(2)$	−41	$\varphi_{xy}(5)$	−195
$\varphi_{yy}(2)$	−198	$\varphi_{yy}(5)$	−6
$\varphi_{xx}(3)$	742	$\varphi_{zz}(5)$	17
$\varphi_{yy}(3)$	284	$\varphi_{xy}(5)$	−71
$\varphi_{yz}(3)$	153	$\varphi_{xy}(6)$	−137
$\varphi_{xz}(3)$	306	$\varphi_{yz}(6)$	−135

tentials. This is the approach used in the derivation of the general form of the APW matrix element by Golibersuch[10] and Sinha.[11] Allen and Lee[12] later demonstrated that the APW matrix element can be expressed in terms of a pseudopotential which depends only on a set of phase shifts $\eta_l(E_F)$. These phase shifts can be determined by fitting de Haas–van Alphen data to a phase-shift model of the Fermi surface, and are those that are used in our calculations of the shape of the Fermi surface.

The phase shifts so determined depend on an energy parameter E_F, which is equal to the depth of the constant interstitial potential as measured from the Fermi energy. The phase shifts can be fitted to experimental data over a wide range of E_F.[17] The small-angle scattering limit of the potential, however, varies linearly with the energy parameter E_F, and the appropriate choice of the energy parameter can be derived by long-wavelength screening considerations. Ziman[18] has shown that, in the limit of long wavelengths, the pseudopotential must have the form

$$\lim_{\vec{q}\to 0} V_{\mathrm{APW}}(\vec{q}) = \frac{-1}{D(\epsilon_F)} , \tag{13}$$

where $D(\epsilon_F)$ is the density of states at the Fermi energy. This limit then uniquely defines the energy parameter E_F and the corresponding set of phase shifts.

Following the discussion of Golibersuch and later Allen and Lee, we write the electron-phonon matrix element as

$$M_{\vec{k}\vec{k}'} = \langle \vec{k}' | \sum_j \delta\vec{R}_j \cdot \frac{\partial U}{\partial \vec{R}_j}\bigg|_{R_j=R_j^0} | \vec{k} \rangle , \tag{14}$$

where the summation is over all lattice sites. $|\vec{k}\rangle$ is the APW wave function which is given inside the muffin-tin sphere by

$$|\vec{k}\rangle = \sum_{\vec{G}} \alpha_{\vec{G}}^{\vec{k}} \Psi(\vec{k}+\vec{G}) , \tag{15a}$$

where

$$\Psi(\vec{k}) = \sum_{l,m} C_{l,m}(\vec{k}) u_l(r) Y_{l,m}(\hat{r}) . \tag{15b}$$

The $u_l(r)$ are the solutions of the radial Schrödinger equation, $Y_{l,m}$ are spherical harmonics, and the $C_{l,m}(\vec{k})$ are given by

$$C_{l,m}(\vec{k}) = 4\pi i^l Y_{l,m}^*(\hat{k}) j_l(kR_s)/u_l(R_s) ,$$

where $j_l(kR_s)$ is the lth-order spherical Bessel function. In the interstitial region $r > R_s$, where R_s is the muffin-tin radius, the $\Psi(\vec{k})$ are plane waves:

$$\Psi(\vec{k}) = e^{i\vec{k}\cdot\vec{r}} . \tag{16}$$

(Note that we are only considering the problem of one atom per primitive unit cell.)

The potential U appearing in Eq. (14) is a muffin-tin potential, with the gradient outside the muffin tin taken to be zero. This potential is described by a set of phase shifts $\eta_l(E_F)$. Lee and Heine[17] have pointed out that the proper choice of the phase shifts for the calculation of the electron-phonon matrix element corresponds to a potential which is formed by summing the individual overlapping atomic potentials screened by the conduction electrons, and which they term a pseudoatom pseudopotential. This potential has the required small-angle scattering limit—the inverse density of states at the Fermi energy.

The deviation of the ionic coordinate $\vec{R}_j$ from its equilibrium value $\vec{R}_j^0$ can be expressed in terms of phonon creation and annihilation operators by

$$\delta\vec{R}_j = \sum_{\vec{q},\sigma} \left(\frac{\hbar}{2NM\omega_q^\sigma}\right)^{1/2} \hat{\epsilon}_{q\sigma} e^{i\vec{q}\cdot\vec{R}_l^0} (a_{-\vec{q}\sigma}^\dagger + a_{\vec{q}\sigma}) , \tag{17}$$

where M is the ionic mass, ω_q^σ is the phonon frequency of wave vector q and polarization σ, N is the number of atoms per unit volume, and $\hat{\epsilon}_{q\sigma}$ is the unit polarization vector. Thus the evaluation of the matrix element reduces to the evaluation of the quantity $\hat{\epsilon}_{q\sigma}\cdot\vec{I}(\vec{k},\vec{k}')$, where

$$\vec{I}(\vec{k},\vec{k}') = \langle \vec{k}' | \nabla U | \vec{k} \rangle . \tag{18}$$

In Eq. (18), $|\vec{k}\rangle$ is a single APW. Allen and Lee have shown that the above equation can be reduced to

$$\hat{z}\cdot\vec{I}(\vec{k},\vec{k}') = (4\pi)^2 i \sum_l F(l) \sum_m \left(\frac{(l+1)^2-m^2}{(l+1)^2}\right)^{1/2} \times \left(\frac{A_l}{u_l u_{l+1}} Y_{l+1,m}^*(\hat{k}) Y_{l,m}(\hat{k}') - \frac{B_l}{u_l u_{l+1}} Y_{l,m}^*(\hat{k}) Y_{l+1,m}(\hat{k}') \right) , \tag{19}$$

where

$$B_l = j_{l+1}(k'R_s) j_l(kR_s) , \quad A_l = j_l(k'R_s) j_{l+1}(kR_s) ,$$

$$u_l = j_l(\kappa R_s) - \tan\eta_l(E_F)\, y_l(\kappa R_s) , \quad \kappa = E_F^{1/2} .$$

j_l and y_l are the spherical Bessel and Neumann functions, respectively, and $F(l)$ is given by

$$F(l) = \frac{1}{\Omega}\left(\frac{l+1}{(2l+1)(2l+3)}\right)^{1/2} \times [\tan\eta_l(E_F) - \tan\eta_{l+1}(E_F)] , \tag{20}$$

where $\eta_l(E_F)$ are the APW phase shifts. Allen and Lee were concerned with the electron-phonon interaction in the alkali metals, of which the Fermi surfaces are essentially spherical, and they evaluated Eq. (19) in the case $|\vec{k}| = |\vec{k}'|$. In this paper Eq. (19) is evaluated without this restriction.

By making use of the addition theorem for spherical harmonics and by successive use of the recursion relation

TABLE II. Energy derivative of the logarithmic derivative of the radial wave function in copper, I_ν^l (in atomic units), as defined in Eq. (25).

$l=0$	1.1154
$l=1$	0.6529
$l=2$	26.7646
$l=3$	0.3249
$l=4$	0.2286
$l=5$	0.1911
$l=6$	0.1644
$l=7$	0.1443
$l=8$	0.1287

$$\cos\theta\, Y_{l,m} = \left(\frac{(l+1+m)(l+1-m)}{(2l+1)(2l+3)}\right)^{1/2} Y_{l+1,m} + \left(\frac{(l+m)(l-m)}{(2l+1)(2l-1)}\right)^{1/2} Y_{l-1,m} ,$$

we obtain the following result:

$$\vec{I}(\vec{k},\vec{k}') = \frac{4\pi i}{\Omega} \sum_l \frac{\tan\eta_l(E_F) - \tan\eta_{l+1}(E_F)}{u_l\, u_{l+1}} \times \sum_{l'\le l} \tfrac{1}{2}\left[(A_l + B_l)(\hat{k} - \hat{k}') + (-)^{l+l'}(A_l - B_l)(\hat{k} + \hat{k}')\right] \times (2l'+1) P_{l'}(\cos\theta_{\vec{k}\vec{k}'}) . \quad (21)$$

Thus, the APW matrix element is given by

$$M^\sigma_{\vec{k}\vec{k}'} = \left(\frac{\hbar}{2MN\omega_q^\sigma}\right)^{1/2} \sum_{\vec{G}\vec{G}'} \alpha^{\vec{k}}_{\vec{G}}\, \alpha^{\vec{k}'}_{\vec{G}'}\, \vec{I}(\vec{k}+\vec{G}, \vec{k}'+\vec{G}') . \quad (22)$$

The expansion coefficients $\alpha^{\vec{k}}_{\vec{G}}$, $\alpha^{\vec{k}'}_{\vec{G}'}$ appearing in the above equation, are those of the normalized eigenfunctions of the APW secular determinant. The normalization condition on the wave function is

$$\sum_{\vec{G},\vec{G}'} \int_{\text{cell}} \alpha^{\vec{k}}_{\vec{G}}\, \alpha^{\vec{k}'}_{\vec{G}'}\, \Psi^*(\vec{k}+\vec{G})\, \Psi(\vec{k}'+\vec{G}')\, d\vec{r} = \Omega , \quad (23)$$

where Ω is the volume of the unit cell. The overlap integral is given by

$$\int \Psi^*(\vec{k}+\vec{G})\, \Psi(\vec{k}+\vec{G}')\, d\vec{r} = \Omega\delta_{\vec{G}\vec{G}'} - 4\pi R_s^2 \frac{j_l(R_s|\vec{G}-\vec{G}'|)}{|\vec{G}-\vec{G}'|} \sum_l (2l+1) P_l(\cos\theta_{k+G,\,k+G'}) \times j_l(R_s|\vec{k}+\vec{G}|)\, j_l(R_s|\vec{k}+\vec{G}'|)\, I_\nu^l , \quad (24)$$

where, following Loucks,[19] we have defined I_ν^l as the energy derivative of the logarithmic derivative of the radial wave function

$$I_\nu^l = -\frac{\partial}{\partial E} \frac{u_l'(R_s,E)}{u_l(R_s,E)} . \quad (25)$$

Equation (25) was evaluated by solving the Schrödinger equation for an empirical nonlocal modification of the Chodorow potential.[20] The results for I_ν^l are presented in Table II.

In calculations of the band structure and of the shape of the Fermi surface, it is necessary to use at least 30 basis functions to obtain a good fit to experimental data. In calculations of the electron-phonon interaction, however, it is possible to obtain agreement with experiment using far fewer basis functions. Allen and Lee, in their work on the phonon resistivities of the alkalis, obtain satisfactory results using single-APW basis functions. In the alkalis the Fermi surface is essentially free-electron-like, and one expects a single plane wave to be a good approximation to the wave function, whereas in copper the Fermi surface protrudes to intersect the zone boundary. Near the zone boundary the wave function can only be described by a mixture of APW basis functions.

In the present work the matrix elements were calculated using wave functions involving from 2 to 30 APW basis functions. The choice of a reduced set of basis functions was made by solving the APW secular determinant for the normalized wave function using a 60-APW expansion at each of the points of interest. A set of basis functions with the largest coefficients was then chosen, and the reduced secular determinant was solved for the normalized wave function. When a reduced set of basis functions is used for the wave-function expansion, the APW secular determinant is, in general, no longer zero; therefore a least-squares procedure was used to solve the reduced APW secular determinant for the wave-function coefficients. The errors involved in this truncation procedure are discussed in Sec. IV.

The alternative procedure of approximating the wave function by the leading coefficients of a 60-APW expansion has two drawbacks. The approximate wave function is not properly normalized, and convergence of the electron-phonon matrix element is less rapid. These problems are greatest in a two- or three-basis-function approximation and diminish rapidly as one increases the number of basis functions.

$q \to 0$ *limit of matrix element.* As discussed earlier, it is necessary that the APW pseudopotential should satisfy the appropriate low-q limit. This may be achieved by choosing the parameter E_F so that the following equation is satisfied:

$$\int \frac{dS_{\vec{k}}}{v_{\vec{k}}} \left| \lim_{\vec{q}\to 0} \sum_{\vec{G}\vec{G}'} \alpha^{\vec{k}}_{\vec{G}}\, \alpha^{\vec{k}}_{\vec{G}'}\, \vec{I}(\vec{k}+\vec{G}, \vec{k}+\vec{G}'+\vec{q}) \right| \Big/ \int \frac{dS_{\vec{k}}}{v_{\vec{k}}} = \frac{-1}{D(\epsilon_F)} . \quad (26)$$

[For copper $1/D(\epsilon_F)$ is equal to 0.272 Ry.] The term in the absolute value sign can be expressed in symmetric form as follows:

TABLE III. Set of phase shifts for which the Fermi-surface average of the small-angle scattering limit is equal to the inverse density of states. The energy parameter is expressed in rydbergs and the phase shifts are in radians.

$\eta_0 = 0.732705$	$\eta_2 = -0.025083$
$\eta_1 = 0.233972$	$\eta_3 = 0.000053$
$E_F = 0.27$	

$$|\cdots| = \frac{1}{2} \sum_{\vec{G}\vec{G}'} \alpha^{\vec{k}}_{\vec{G}} \alpha^{\vec{k}}_{\vec{G}'} [\vec{I}(\vec{k}+\vec{G}, \vec{k}+\vec{G}'+\vec{q}) + \vec{I}(\vec{k}+\vec{G}', \vec{k}+\vec{G}+\vec{q})] ,$$

where in the limit $q \to 0$ we have, from Eq. (21),

$$|\cdots| = \frac{1}{2} \sum_{\vec{G},\vec{G}'} \alpha^{\vec{k}}_{\vec{G}} \alpha^{\vec{k}}_{\vec{G}'} \frac{4\pi i}{\Omega} \sum_{l} \frac{\tan\eta_l(E_F) - \tan\eta_{l+1}(E_F)}{u_l u_{l+1}} \times \sum_{l' \leq l} \vec{Q}_{l'}(\vec{k}+\vec{G}, \vec{k}+\vec{G}', \vec{q})(2l'+1) P_{l'}(\cos\theta_{\vec{k}+\vec{G},\vec{k}+\vec{G}'}) . \quad (27)$$

Q is given by

$$\vec{Q}_l(\vec{k}, \vec{k}', \vec{q}) = \left[\frac{\vec{q}^{\,k}_{\perp}}{k} + \frac{\vec{q}^{\,\vec{k}'}_{\perp}}{k'} + (\hat{k} - \hat{k}') \left(q^{k}_{\parallel} \frac{\partial}{\partial k} - q^{k'}_{\parallel} \frac{\partial}{\partial k'} \right) \right] \times \frac{(A_l + B_l)}{2} + (-1)^{l+l'} \left[\frac{\vec{q}^{\,k}_{\perp}}{k} - \frac{\vec{q}^{\,k'}_{\perp}}{k'} + (\hat{k} + \hat{k}') \times \left(q^{k}_{\parallel} \frac{\partial}{\partial k} - q^{k'}_{\parallel} \frac{\partial}{\partial k'} \right) \right] \frac{A_l - B_l}{2} , \quad (28)$$

where $q^k_{\parallel}$, $\vec{q}^{\,k}_{\perp}$ are given by

$$q^k_{\parallel} = \vec{q} \cdot \hat{k} , \quad \vec{q}^{\,k}_{\perp} = \vec{q} - \vec{q} \cdot \hat{k} \hat{k} .$$

The term on the left-hand side in Eq. (26) is approximately a linear function of the energy parameter E_F. Thus it is a simple matter to calculate the appropriate value of E_F and the corresponding phase shifts $\eta_l(E_F)$ that will satisfy Eq. (26).

On the belly of the Fermi surface the difference vector $\vec{q} = \vec{k} - \vec{k}'$ is approximately perpendicular to $\vec{k}$ and $\vec{k}'$, and the small-angle scattering limit is independent of the orientation of $\vec{q}$. Near the neck, however, the matrix element depends on the orientation of $\vec{q}$ with respect to $\vec{k}$ and $\vec{k}'$, and it is necessary to consider the angular average of Eq. (27) when computing the Fermi-surface average of the small-angle scattering limit.

Equation (27) is also the matrix element that enters into the calculation of the relaxation time. As noted before, when $\vec{q}$ is not perpendicular to $\vec{k}$, the matrix element allows for coupling with transverse phonons even in the small-angle scattering limit. It is the aspherical character of the Fermi surface that accounts for the large increase in the scattering rate on the necks over that on the belly. However, the angular average of the transverse component of the matrix element is zero, and hence the Fermi-surface average of the small-angle scattering limit depends only on the longitudinal component of the matrix element.

IV. RESULTS AND DISCUSSION

The Fermi-surface integrals appearing in Eqs. (5) and (26) were evaluated by dividing the Fermi surface into 912 sections of approximately equal area. The integrals were then replaced by a summation over the individual sections. The technique used in the calculation of the area of the individual sections will be reported in Ref. 21.

A. Small-Angle Scattering Limit

Since, as discussed in Sec. III, the Fermi-surface average of the small-angle scattering limit is approximately a linear function of E_F, the value of E_F for which Eq. (26) is satisfied can readily be obtained. The set of phase shifts corresponding to this value of E_F is set out in Table III. Whereas in ordinary pseudopotential theory the small-angle scattering limit is isotropic, the present formulation yields a distinctly anisotropic limit as shown in Fig. 1.

It is important to note that the energy parameter E_F is determined by requiring that the pseudopotential should satisfy the small-angle scattering limit, and that there are no free parameters in the APW formulation of the electron-phonon matrix element.

B. Renormalization

In the calculation of the renormalization factor $\lambda(\vec{k})$, the integral in Eq. (5) was replaced by a summation over 912 sections of the Fermi surface and is given by

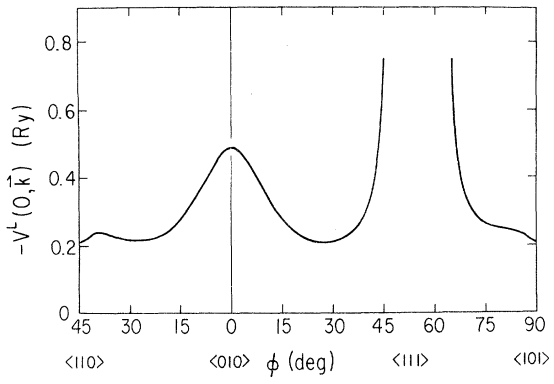

FIG. 1. Small-angle scattering limit of the APW pseudopotential is plotted in symmetry zones of copper. The Fermi-surface average of this limit is -0.272 Ry.

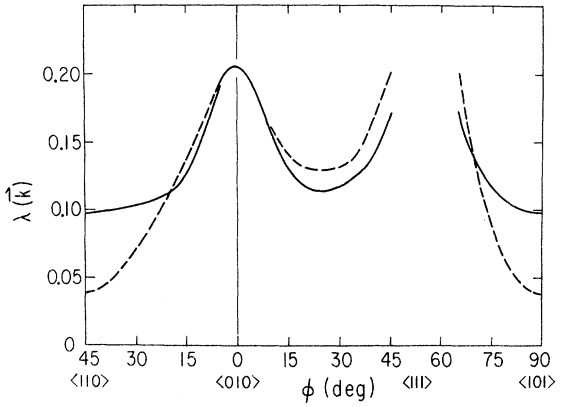

FIG. 2. Angular variations of the electron-phonon renormalization $\lambda(\vec{k})$ in symmetry zones of copper. The solid curve is from the present work and the dotted curve represents Lee's interpretation of experimental cyclotron-mass data.

$$\lambda(\vec{k}) = \frac{2\Omega}{(2\pi)^3} \sum_{i,\sigma} \frac{\Delta S_{\vec{k}_i}}{\hbar v_{\vec{k}_i}} \frac{|M^{\sigma}_{\vec{k},\vec{k}_i}|^2}{\hbar\omega^{\sigma}_{\vec{k},\vec{k}_i}} \quad . \tag{29}$$

This expression was evaluated using three different expansions of the wave function. The first two were mixtures of two or three and three or four basis functions, respectively, while the third was an 8-APW basis-function expansion of the wave function. The Fermi-surface averages of the the enhancement $\langle\lambda(\vec{k})\rangle$ were found to be equal, within the computational error, for all three.

The results of the calculation of $\lambda(\vec{k})$ are presented in Figs. 2 and 3. In Fig. 2 we have plotted contours of constant λ. These were determined by fitting a cubic harmonic expansion to calculated values of λ at the individual points. In Fig. 3 the renormalization factor $\lambda(\vec{k})$ is plotted within symmetry zones and, as can be seen from the plot, λ has maxima along the $\langle 111\rangle$ and $\langle 010\rangle$ directions and a minimum along $\langle 110\rangle$. This is consistent with the anisotropy of $\lambda(\vec{k})$ as obtained from the interpretation of experimental cyclotron-mass data by Lee, also given on the same plot. There are discrepancies, however, in the absolute magnitude of $\lambda(\vec{k})$ along the $\langle 110\rangle$ and $\langle 111\rangle$ directions.

TABLE IV. Result of this paper for the Fermi-surface average of the electron-phonon renormalization is presented, along with other calculated values.

Grimvall (Ref. 24)	0.07 (lower bound)
	0.24 (upper bound)
Nowak and Lee (Ref. 21)	0.10±0.01
Allen (Ref. 6)	0.45 (HM)
	0.08 (FC)
Present work	0.12±0.02

The technique used by Lee to estimate $\lambda(k)$ involves a calculation of the quasiparticle velocities from experimental cyclotron-mass data, and a comparison with the band velocities derived from a modified Chodorow potential, which is believed to include the dominant effects of the electron-electron interaction. Evidence for this assumption has been discussed by Nowak and Lee,[21] and it is further supported by recent work of Williams, Janak, and Moruzzi,[22] who found that the Chodorow potential predicts values of the dielectric function and the energy distribution of photoemitted electrons in good agreement with experimental data. However, Christiensen[23] has stressed the possibility that the Chodorow potential may be less than fully renormalized by the electron-electron interaction. If this is so, Lee's calculation might underestimate $\lambda(\vec{k})$. It is also possible that the discrepancies noted above could arise from uncertainties in the interpretation of the experimental data along various orbits to yield local values of the quasiparticle velocity.

The Fermi-surface average of $\lambda(\vec{k})$ was obtained by summing the individual $\lambda(\vec{k})$ weighted by the local area and density of states. This average $\langle\lambda\rangle$ is given in Table IV, together with estimates by other authors. The theoretical estimates of the upper and lower bounds on $\langle\lambda\rangle$ were calculated by Grimvall[24] from superconductivity data and resistivity data, respectively. Allen's[6] results were based on first-principles calculations, utiliz-

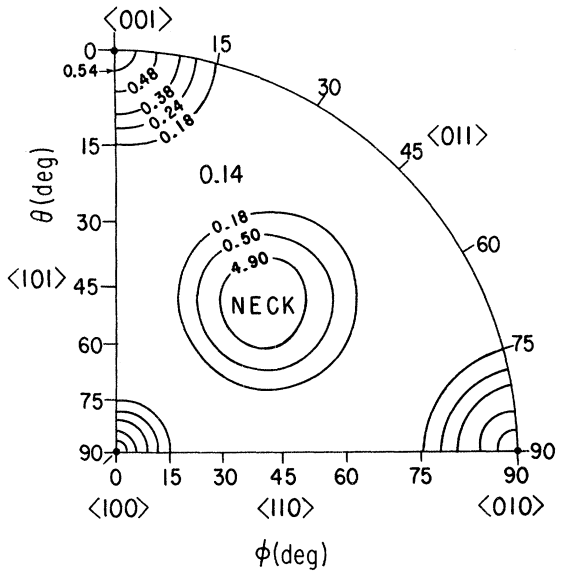

FIG. 3. Contours of the electron-phonon renormalization $\lambda(\vec{k})$ in copper are plotted on a stereographic projection. The contours were obtained from a cubic-harmonic expansion fitted to the results calculated at selected points on the Fermi surface.

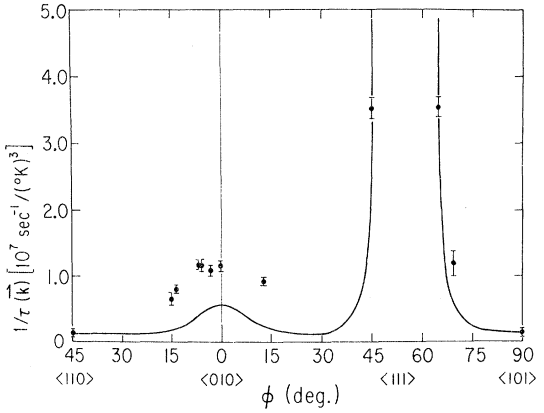

FIG. 4. Angular variations of the inverse relaxation time $1/\tau(\vec{k})$ in symmetry zones of copper. The solid curve is from the present work, and the points represent the experimental data of Koch and Doezema. On the belly of the Fermi surface the experimental points represent averages over an angular range of about ±6°.

ing a one-plane-wave expansion for the wave function and assuming a spherical Fermi surface. The two values he reports are calculated from the Harrison–Moriarty (HM) pseudopotential[25] and the Fong-Cohen (FC) pseudopotential,[7] respectively. Allen decomposed the HM and FC potentials in terms of effective phase shifts, and found that the d-phase shift is negative in the HM pseudopotential, but is positive in the FC pseudopotential. A negative d-phase shift corresponds to a repulsive interaction due to the d bands lying below the Fermi surface, and is in agreement with scattering theoretical arguments. The value of Nowak and Lee[21] was obtained by an approach similar to that used by Lee in his analysis of the anisotropy of the renormalization.

C. Relaxation Time

The relaxation time was calculated from Eq. (9). The procedure is quite straightforward on the belly of the Fermi surface where the small-angle scattering limit is very nearly independent of the orientation of $\vec{q}$, and the matrix element involves terms coupled only by longitudinal phonons. Equation (9) was evaluated by setting $C^L = 4.69 \times 10^5$ cm sec^{-1} and calculating $|M^L_{\vec{k}\vec{k}}|^2$, using a 30-APW basis-function approximation to the wave function. Near the necks, however, the problem must be treated more carefully. To calculate the relaxation time, it is necessary to calculate $\hbar/\tau(\vec{k})$ for all possible orientations of $\vec{q}$, since for arbitrary $\vec{q}$, coupling to transverse phonons is possible. This was accomplished by dividing the plane of $\vec{q}$ into intervals of $\frac{1}{20}\pi$ radians and then calculating $|M^\sigma_{\vec{k}\vec{k}}|^2$ and C_σ in each of the intervals. The results of this calculation within symmetry zones are shown in Fig. 4, together with the experimental data of Koch and Doezema.[2] A plot of the contours of constant τ is given in Fig. 5. These were obtained by the same technique as for the renormalization.

TABLE V. Present results for the orbital average of the inverse relaxation time on the belly, $1/\tau_B$, and on the "dog's bone" orbit, $1/\tau_D$, are compared with preliminary experimental data of Gantmakher.

	$1/\tau_B$	$1/\tau_D$
	(10^7 sec^{-1}/°K^3)	
Gantmakher (Ref. 3)	0.3	0.67
Present work	0.23 ± 0.05	0.67 ± 0.17

Our results can be compared with the experimental data of Koch and Doezema, and agree with the general form of the anisotropy they report, although our calculations yield a value smaller than the experimental value near the ⟨100⟩ symmetry direction. Also, their result on the neck is slightly smaller than ours. Gantmakher[3] has measured the inverse relaxation time averaged around the belly orbit normal to ⟨100⟩, $1/\tau_B$, and around the "dog's bone" orbit, $1/\tau_D$. His results are shown in Table V, together with the corresponding averages from the present work. Our results are consistent with the experimental value for $1/\tau_D$; however, our value for $1/\tau_B$ is somewhat smaller than the reported experimental value. This may be because our results underestimate the absolute magnitude

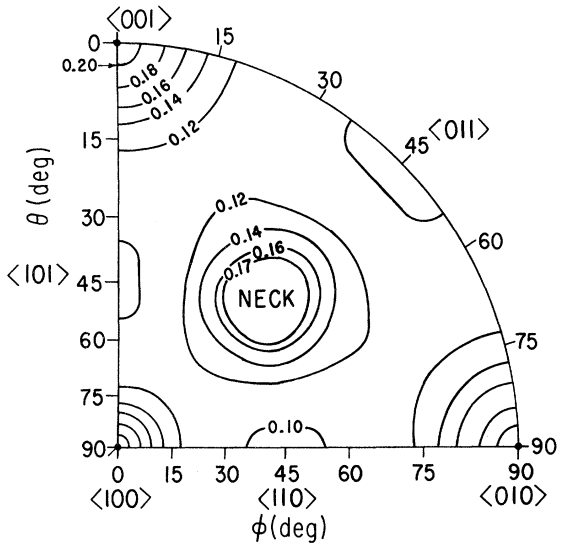

FIG. 5. Contours of the inverse relaxation time $1/\tau(\vec{k})$ in copper are plotted on a stereographic projection. The contours were obtained from a cubic-harmonic expansion fitted to the results calculated at selected points on the Fermi surface. The contours are in units of 10^7 sec^{-1}/°K^3.

of the scattering rate near the ⟨100⟩ direction, as is suggested by a comparison with the results of Koch and Doezema.

The error involved in the truncation of the wave functions can be estimated by checking the convergence of the matrix element as the number of basis functions is increased. In the small-angle scattering limit, the change in going from 8 to 30 basis functions is less than 10% in the local matrix elements and less than 5% in the Fermi surface average of the matrix element.

The uncertainties associated with the results reported in this paper do not reflect any errors involved in replacing the actual lattice potential with displaced "muffin tins." As discussed above, the choice of the muffin-tin-potential approach was motivated by the success of this method for energy-band calculations, particularly in the transition metals, and for discussion of the phonon resistivities of the alkali metals. The expression for the electron-phonon matrix element used in the present paper involves the replacement of the perturbed lattice potential by an array of rigidly displaced potentials of muffin-tin form. Sinha[11] has derived an expression for the electron-phonon matrix element which includes the present result plus additional terms representing the electron response. The form of the electron-phonon matrix element used in the present calculations is the dominant term, and calculations by S. T. Chui suggest that the additional terms are an order of magnitude smaller.[26] The small-angle scattering limit [Eq. (13)] applies strictly to the complete electron-matrix element, and to this extent the determination of E_F and the phase shifts is approximate.

V. CONCLUSION

In the present paper the application of the APW method to the problem of calculating the anisotropy of the electron-phonon renormalization and the temperature-dependent (T^3) component of the quasiparticle relaxation time is discussed. This approach requires a knowledge of the anisotropies of the Fermi surface and the phonon spectrum. The matrix elements of the electron-phonon interaction were calculated from an APW pseudopotential, involving phase shifts determined by an analysis of experimental Fermi-surface data. The wave functions used in the evaluation of the electron-phonon matrix element were determined by diagonalizing the APW secular determinant. Such an approach yields absolute values of the renormalization and relaxation time.

The renormalization is in good over-all agreement with results obtained by Lee from an analysis of experimental cyclotron-mass data. The scattering rate is also in good agreement with experimental data of Koch and Doezema. This success in describing the principal features of the anisotropy of the electron-phonon interaction in copper suggests that the APW pseudopotential may prove to be an accurate way of describing the electron-phonon interaction in transition metals.

ACKNOWLEDGMENTS

The author would like to express his appreciation to Martin J. G. Lee, who suggested this problem, for his constant help and encouragement, and to Philip B. Allen for several helpful comments.

---

*Work supported in part by facilities provided by the Advanced Research Projects Agency for Materials Research at the University of Chicago.

†This paper will be submitted to the University of Chicago in partial fulfillment of the requirements for the Ph. D. degree.

[1]P. Häussler and S. J. Welles, Phys. Rev. 152, 675 (1966).

[2]J. F. Koch and R. E. Doezema, Phys. Rev. Letters 24, 507 (1970); and private communication.

[3]V. F. Gantmakher (private communication).

[4]M. Springford, Advan. Phys. 20, 493 (1971).

[5]M. J. G. Lee, Phys. Rev. B 2, 250 (1970).

[6]P. B. Allen, Phys. Rev. B 5, 3857 (1972).

[7]C. Y. Fong and M. L. Cohen, Phys. Rev. Letters 24, 306 (1970).

[8]M. J. G. Lee, Phys. Rev. 187, 901 (1969); see also Ref. 21.

[9]R. M. Nicklow, G. Gilat, H. G. Smith. L. J. Raubenheimer, and M. K. Wilkinson, Phys. Rev. 164, 922 (1967).

[10]D. C. Golibersuch, Phys. Rev. 157, 532 (1967).

[11]S. K. Sinha, Phys. Rev. 169, 477 (1968).

[12]P. B. Allen and M. J. G. Lee, Phys. Rev. B 5, 3848 (1972).

[13]See, for example, D. Pines, *Solid State Physics* (Academic, New York, 1955), Vol. 1.

[14]A. B. Migdal, Zh. Eksperim. i Teor. Fiz. 34, 1438 (1958) [Sov. Phys. JETP 7, 966 (1958)].

[15]G. M. Eliashberg, Zh. Eksperim. i Teor. Fiz. 38, 966 (1960) [Sov. Phys. JETP 11, 696 (1960)]; V. Ambegaokar and L. Tewordt, Phys. Rev. 134, A805 (1964); W. L. McMillan, *ibid.* 167, 331 (1968).

[16]P. B. Allen, in *Proceedings of the Twelfth International Conference on Low Temperature Physics, Kyoto,* 1970, edited by E. Kanda (Academic Press of Japan, Tokyo, 1970), p. 517.

[17]V. Heine and M. J. G. Lee, Phys. Rev. Letters 27, 811 (1971); M. J. G. Lee and V. Heine, Phys. Rev. B 5, 3839 (1972).

[18]J. M. Ziman, *Electrons and Phonons* (Oxford U. P., Oxford, England, 1960).

[19]T. L. Loucks, *Augmented Plane Wave Method* (Benjamin, New York, 1967).

[20]M. J. G. Lee (unpublished).

[21]D. Nowak and M. J. G. Lee, Phys. Rev. B 5, 2851 (1972).

[22]A. R. Williams, J. F. Janak, and V. L. Moruzzi,

Phys. Rev. Letters 28, 671 (1972).
[23]N. E. Christiensen, Solid State Commun. 9, 749 (1971).
[24]G. Grimvall, Physik Kondensierten Materie 11, 279 (1970).
[25]J. Moriarty, Phys. Rev. B 1, 1363 (1970).
[26]S. K. Sinha (private communication).

PHYSICAL REVIEW B VOLUME 6, NUMBER 10 15 NOVEMBER 1972

Electronic Phase Transitions of Cerium Metal*

Miguel Kiwi
Facultad de Ciencias, Universidad de Chile, Casilla 653, Santiago, Chile

and

Ricardo Ramírez
Instituto de Física, Universidad Católica de Chile, Casilla 114-D, Santiago, Chile
(Received 12 January 1972)

The model recently proposed by Ramírez and Falicov is generalized by the incorporation of the spin-orbit splitting of the $4f$ shell. This generalization provides an understanding of the fractional valence and magnetic susceptibility of α-cerium and suggests a mechanism to drive the α-α' phase transition.

I. INTRODUCTION

Phase transitions of Ce metal have received a great deal of attention in recent publications.[1-3] A p-T phase diagram (as given in Refs. 2 and 3) shows the following most relevant properties of the different forms Ce metal takes: The β and γ phases exhibit a magnetic moment close to the value of a singly occupied $4f$ shell. The α phase shows about one-fourth of the magnetic susceptibility of the γ phase,[1] while the α' phase has been found to be superconducting,[4] which implies that it has very weak magnetic properties. On the other hand, the β phase undergoes an antiferromagnetic transition at 12.5 °K making Ce the only known element to have both magnetic and superconducting phases.[1]

In this paper we also focus our attention on the α-α' phase transition for which the available experimental knowledge can be summarized as follows: (a) At room temperature the transition is observed[2] to occur at about 50 kbar; (b) the superconducting transition temperature[4] is 1.8 °K; (c) there is no agreement with regard to the crystal structure of the α' phase,[2] but the lattice parameter has been determined as 4.66 Å, while the α phase is known to be fcc with a lattice constant of 4.73 Å; and (d) the α phase has a valence of 3.67 ± 0.09, intermediate between the γ-phase value of about 3.0 and the α' phase which is assumed to be a truly four-valent metal.[1]

From the theoretical point of view, Ramírez and Falicov[3] (RF) recently proposed a model to explain the γ-α phase transformation of Ce. They assumed that the transition was driven by the promotion of one electron from an f orbital in the γ phase to the s-d conduction band in the α phase.[3] This implies that the α phase would consist of nonmagnetic Ce^{4+}-ion cores and four conduction electrons per atom, and therefore does not agree completely with the experimental results mentioned above.

In this paper we generalize the RF model in order to achieve a satisfactory agreement with experiment and suggest a mechanism to explain the α-α' phase transition. The main feature of our generalization is to incorporate the spin-orbit splitting of the $4f$ shell into the theory; this is achieved by introducing a doubly peaked density of f states in order to allow electrons to populate both the $J = \frac{5}{2}$ ground state or the $J = \frac{7}{2}$ excited state of the Ce atom.

In a certain way our model incorporates, and provides a formalism for, qualitative ideas outlined by Maple and Wohlleben[5] in relation to SmS, which in turn are based on a recent proposal of Hirst[6]; a discussion of this aspect is given in Sec. IV.

The general outline of this paper is as follows: After the present introduction a significantly improved solution of the RF model is given in Sec. II. On the basis of this solution, the generalized theory, which includes the spin-orbit splitting of the $4f$ shell, is developed in Sec. III. A full account of the minimization procedure of the pertinent forms of the Helmholtz free energy, its evaluation as well as the phase transitions and critical behavior that result, are given both in Secs. II and III. The paper is closed in Sec. IV with a critical discussion of the theory, in the